

# Construction of Uniform Designs over Continuous Domain in Computer Experiments

Jianfa Lai<sup>1</sup>, Kai-Tai Fang<sup>2,3</sup>, Xiaoling Peng<sup>2</sup>, and Yuxuan Lin<sup>\*,2</sup>

## Abstract

Construction of uniform designs (UDs) has received much attention in computer experiments over the past decades, but most of previous works obtain uniform designs over a U-type by lattice domain. Due to increasing demands for continuous factors, UD over continuous domain is in lack. Moreover, the uniformity can be further improved over a continuous domain. In this paper, we use coordinate descent methods with an initialization derived by threshold accepting (TA) algorithm to construct UD over continuous domain with Centered  $L_2$ -discrepancy. The new UD perform better than the recorded ones in several computer experiments by the Kriging modeling.

**Keywords:** Centered  $L_2$ -discrepancy, Computer experiment, Coordinate descent, Kriging modeling, Lattice point, Threshold accepting, Uniform designs

*MSC:* 62K05; 62K15

## 1 Introduction

With the development of science and technology, computer experiments have gained more and more attention in recent years. Engineers and scientists implement com-

---

<sup>1</sup>Department of Mathematics, Hong Kong Baptist University, Kowloon Tong, Hong Kong

<sup>2</sup>Division of Science and Technology, BNU-HKBU United International College, Zhuhai 519085, China

<sup>3</sup>The Key Lab of Random Complex Structures and Data Analysis, The Chinese Academy of Sciences, Beijing, China

puter simulations on physical systems due to the complex relationships between the inputs and outputs. Fang et al. (2005) gave a comprehensive introduction to the design and modeling of computer experiments. In computer experiments, the true underlying model

$$Y = h(X_1, \dots, X_s), \quad (X_1, \dots, X_s) \in \mathcal{T} \quad (1)$$

is known and usually too complicated to conduct some computation demanding works such as sensitivity analysis and optimization, where the response  $Y$  depends on the factors  $X_1, \dots, X_s$  in the experimental domain  $\mathcal{T}$ . For a given input  $\{\mathbf{x}_1, \dots, \mathbf{x}_n\} \in \mathcal{T}$  representing  $n$  experimental runs, one can obtain their output  $\{y_i, i = 1, \dots, n\}$  from the true model (1). Based on the observations of the data set  $\{y_i, \mathbf{x}_i, i = 1, \dots, n\}$ , an approximate model

$$Y = \hat{h}(X_1, \dots, X_s), \quad (2)$$

called *metamodel* is built and used for some applications such as optimization and sensitivity analysis. There are various modeling techniques such as Kriging models, (orthogonal) polynomial regress models, Bayesian methods and neural networks. More details can be found in Fang et al. (2005).

There are two key issues in computer experiments: design and modeling. The so-called space filling design has been recommended for computer experiments. The Latin hypercube sampling (LHS) proposed by McKay et al. (1979) is one of the most popular space filling design. With design points uniformly scattered on the experimental domain, the uniform design proposed by Fang (1980), Wang and Fang (1981) is another widely used space-filling design.

The Latin hypercube sampling and uniform design are based on the estimation of overall mean of  $Y$ :

$$E(Y) = \int_{\mathcal{T}} h(\mathbf{x}) d\mathbf{x} = E(h(\mathbf{x})),$$

where  $\mathbf{x} = (x_1, \dots, x_s)$  follows the uniform distribution on  $\mathcal{T}$ . Then  $E(Y)$  can be estimated by the mean  $\bar{h} = \frac{1}{n} \sum_{i=1}^n h(\mathbf{x}_i)$ . LHS provides a more efficient estimate of  $E(Y)$  than the estimate by the simple random sampling. The Koksma-Hlawka inequality (see Hua and Wang (1981)) gives the upper error bounds of the estimate as

$$|E(h(\mathbf{x})) - \bar{h}| \leq D(\mathcal{P})V(h), \quad (3)$$

where  $V(h)$  is a measure of the variation of  $h$ , and  $D(\mathcal{P})$  is the star-discrepancy of  $\mathcal{P}$ , a measure of the uniformity of  $\mathcal{P}$ . The definition of  $V(h)$  is in the sense of Hardy and Krause (Hua and Wang (1981)). Note that  $V(h)$  is independent of the design points. Thus, given a bounded  $V(h)$ , inequality (3) indicates that the more uniform a set  $\mathcal{P}$  of points is over the experimental region  $\mathcal{T}$ , the more accurate  $\bar{h}$  is as an estimator of  $E(h(\mathbf{x}))$ . The uniform design is based on this overall mean model.

When the factors are quantitative and their domain is a rectangle  $a_i \leq X_i \leq b_i, i = 1, \dots, s$ , without loss of generality, we can assume the experimental domain is a unit cube  $C^s = [0, 1]^S$ . To measure the uniformity, Hickernell (1998) proposed some new discrepancies such as *Centered  $L_2$ -discrepancy* (CD) and *wrap-around  $L_2$ -discrepancy* (WD) to replace the star-discrepancy. Zhou et al. (2013) also suggested *mixture discrepancy* (MD). In this paper, we adopt CD. The squared CD has a computational formula

$$\begin{aligned} CD^2(\mathcal{P}) &= \left(\frac{13}{12}\right)^s - \frac{2}{n} \sum_{i=1}^n \prod_{k=1}^s \left(1 + \frac{1}{2}|x_{ik} - 0.5| - \frac{1}{2}|x_{ik} - 0.5|^2\right) \\ &+ \frac{1}{n^2} \sum_{i=1}^n \sum_{j=1}^n \prod_{k=1}^s \left(1 + \frac{1}{2}|x_{ik} - 0.5| + \frac{1}{2}|x_{jk} - 0.5| - \frac{1}{2}|x_{ik} - x_{jk}|\right), \end{aligned} \quad (4)$$

where  $\mathbf{x}_i = (x_{i1}, \dots, x_{is})$  is from a unit hypercube  $C^s = [0, 1]^s$ . The uniform design is defined as follows.

**Definition 1.** For an experiment consists of  $n$  runs relating to  $s$  factors on an experimental region  $\mathcal{T}$ , denote the experimental domain by  $\mathcal{U}$  that is collection of sets  $\mathcal{P} = \{\mathbf{x}_1, \dots, \mathbf{x}_n\} \in \mathcal{T}$ . Then a design,  $\mathcal{P}^* = \{\mathbf{x}_1^*, \dots, \mathbf{x}_n^*\} \in \mathcal{T}$ , is called a uniform design under a given measure discrepancy  $\mathcal{D}$  if

$$\mathcal{D}(\mathcal{P}^*) = \min_{\mathcal{P} \in \mathcal{U}} \mathcal{D}(\mathcal{P}). \quad (5)$$

Constructing a uniform design is an NP hard problem that there is no exact algorithm for global optima within polynomial time. Besides, in practical experiments, the feasible values of factors are limited so that the corresponding levels in designs are required to be discrete. Therefore, for construction of uniform designs, traditional methods often focused on a lattice domain  $\mathcal{U}$  instead of the full set  $\mathcal{P}$ . The U-type domain is prevalently accepted in existing literatures.

**Definition 2.** Suppose a design  $\mathbf{U}$  is an  $n \times s$  matrix. Then it is said to be a  $q$ -level U-type design denoted as  $\mathbf{U}(n, q^s)$  if in each column of  $\mathbf{U}$ , the entries,  $\frac{l-0.5}{q}$  for  $l = 1, \dots, q$ , appear equally often.

Most of authors restrict a U-type design in an experimental region,  $[0, 1]^s$ , defined in Definition 2. The uniform design obtained from a U-type domain is called U-type uniform design, denoted as  $\mathbf{U}_n(q^s)$ . There are many construction approaches to  $\mathbf{U}_n(q^s)$ , such as the good lattice point method, the combinatorial construction method, cutting method, and the foldover technique. Stochastic optimization algorithm is also feasible for this problem. More details can refer to Fang et al. (2018).

The threshold accepting (TA) algorithm proposed by Dueck and Scheuer (1990), is a variation of the more widely used simulated annealing (SA) algorithm, that proposed by Kirkpatrick (1984) through the emulation of the physical annealing process in solids. However, since SA algorithm involves too many parameters for

the user choosing, its process convergence is slow. Hence in many cases, TA as a descendent has better performance than SA since it provides quicker convergence and better results during the same computational time. Multivariate or combinatorial optimization problems, including some NP-complete or NP-hard problems, have been tackled through TA, such as portfolio optimization problem (Dueck and Winker (1992)), NP-complete problem of optimal aggregation (Chipman and Winker (1995)) and NP-hard traveling salesman problem (Winker (1994)).

Referred to the definition of a uniform design in (5), generating a UD is a large scale integer programming problem with multimodal objective function (*i.e.* discrepancies) over a discrete, large and complicated domain (*i.e.* experimental region). Winker and Fang (1997) and Winker and Fang (1998) firstly applied the TA to the calculation of the star discrepancy and construction of uniform designs on the lattice domain. Fang et al. (2017) discussed how to apply TA to construction of orthogonal designs. Most uniform designs recorded on the website <https://dst.uic.edu.cn/en/isci/uniform-design/uniform-design-tables> have been obtained by TA algorithm.

Computer simulations play a dominant role in modern applications. Traditional computer experimental designs are in a lattice domain, in which the factors of interest are limited with discrete levels in experiments. However, with the improvement of computational ability, factors in practical may refer to a continuous domain, that leads to a great loss of information if the experimenter still choose a design from a lattice domain. The uniform designs over continuous domain are suitable for this case, and easily to be carried out. They should have better uniformity than U-type UDs as well, and as consequence, perform better in modeling. Hence, construction of uniform designs over continuous domain is in badly need. Our paper is to propose an approach to obtaining the UDs over continuous domain, especially in a rectangle. Finding a uniform design in a continuous  $C^s = [0, 1]^s$  is a high dimensional non-convex optimization problems. Here we only consider the case in which  $n = q$

in Definition 2. For a point set  $\mathcal{P} = \{\mathbf{x}_1, \dots, \mathbf{x}_n\} = (x_{ik})_{n \times s}$  from  $C^s = [0, 1]^s$ , the objective is to minimize the square of CD (4):

$$X = \arg \min_{\mathcal{P}} CD^2(\mathcal{P}). \quad (6)$$

Gradient descent (Ruder (2016)) is a good way to solve such problems with a suitable initialization. However, it costs too much for large sized designs (i.e.  $n$  and  $s$  are large), which are prevalent in computer experiments. Coordinate descent (Wright (2015)) is also feasible for this problem. Compared with gradient descent, the coordinate update is simpler and cheaper, especially for the high dimensional optimization problems. Choosing a suitable initial design is very important, in this paper we adopt initial designs obtained from TA. An introduction of TA algorithm is given in Section 2. In Section 3, the implementation on constructing uniform designs through coordinate descent methods are conducted, in which iteration formula of CD is feasible to facilitate the efficiency of algorithm. To evaluate the modeling performance of new uniform designs over continuous domain, we adopt several case studies of computer experiments in Section 4.

## 2 Constructing Uniform Designs through TA Algorithm

The TA algorithm starts with an arbitrarily generated U-type design, say  $\mathbf{U}^0(n, q^s)$ , and then it performs a large number of iterations. During each iteration, a new solution is generated and used for substituting the current solution, say  $\mathbf{U}^c(n, q^s)$ , while in the first iteration  $\mathbf{U}^c(n, q^s) = \mathbf{U}^0(n, q^s)$ . The new solution  $\mathbf{U}^{new}(n, q^s)$  is derived from a so-called *neighborhood* of the current solution  $\mathbf{U}^c(n, q^s)$ , which is often defined as a small permutation of the current solution. A decision rule in each iteration is to determine whether to accept the new solution and update the

current objective function value or not. We present the flow chart of TA algorithm for generating uniform designs in Figure 1.

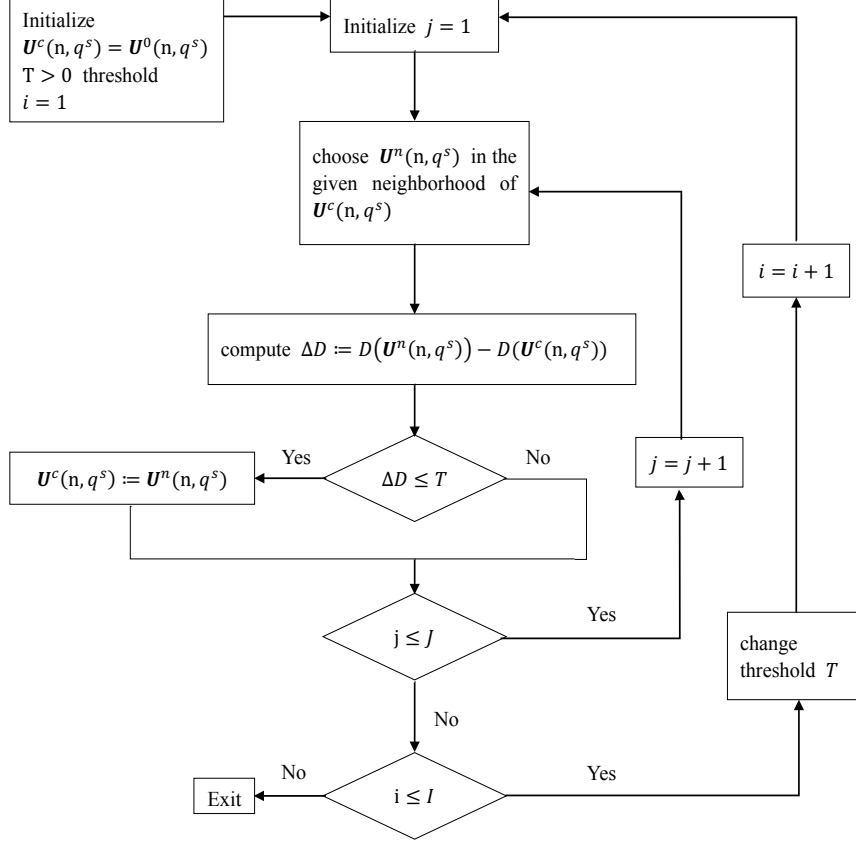


Figure 1: Threshold Accepting Algorithm for Generating Uniform Designs

In uniform design construction, the purpose is to minimize the discrepancy. Hence, in each iteration, the results of the new candidate and the current solution are compared through  $\Delta D = D(\mathbf{U}^c(n, q^s)) - D(\mathbf{U}^{new}(n, q^s))$ . A trivial local search algorithm accepts  $\mathbf{U}^{new}(n, q^s)$  if and only if  $\Delta D \geq 0$ . In this algorithm, the resulting solution has a large probability that gets stuck in a bad local optimum especially as the objective function is multimodal. Winker and Fang (1998) indicated that in the application to the traveling salesman problem, the result quality of the trivial local search algorithm got stuck in a bad level and could not be improved by further increasing the number of iterations. Therefore, TA adopts another acceptance

criterion that allows certain temporary worsening with respect to a predetermined threshold value, say  $T \geq 0$ . That implies in each iteration, a new candidate is accepted if and only if  $\Delta D \leq T$ . Thus TA is also regarded as the refined local search algorithm.

The threshold value is not a constant but a finite sequence that is positive and decreasing to zero. As the threshold value is nonzero in most of the iterations, even if the current solution is stuck in a bad local optimum, it has chance to leave. At the very end, the threshold value ends up at zero, that ensures the solution of TA algorithm is still a local optimum. But the local optimum of TA has high quality and at least is approaching to the global optimum.

The key of TA algorithm is to define the neighborhood and threshold sequence. A U-type design is regarded as a neighborhood of the current design if they differ by elements in at most  $k \leq s$  columns. Many authors set  $k = 1$ , and define each neighborhood by randomly exchanging two elements in a randomly chosen column of the current design (so-called TA neighborhood). The definition of the neighborhoods provides an endogenous data-driven approach to generating a threshold sequence. In this paper, we adopt a recursive formula

$$T_i = \frac{I - i}{I} \times T_{i-1}$$

to derive the threshold sequence in an exponentially decreasing manner, refer to Fang et al. (2017). With the given parameters  $\alpha \in (0, 1)$ ,  $I$  and  $J$ , the procedure of generating a threshold sequence is as follows:

- (1) generate the initial design of the TA algorithm,  $\mathbf{U}^0(n, q^s)$ ;
- (2) find  $J$  neighborhoods of the initial design,  $\mathbf{U}^j(n, q^s)$ ,  $j = 1, \dots, J$ ;
- (3) calculate the squared CD values for each neighborhood,  $CD^2(\mathbf{U}^j(n, q^s))$ ;
- (4) compute the range of the squared CD values of the  $J$  neighborhoods,



$range(CD^2(\mathbf{U}^j(n, q^s)));$

(5) set threshold basis  $T_0 = range(D(\mathbf{U}^j(n, q^s))) \times \alpha$  and  $T_1 = \frac{I-1}{I} \times T_0$ ;

(6) generate the rest threshold sequence through  $T_i = \frac{I-i}{I} \times T_{i-1}, i = 2, \dots, I$ .

However, the definition of TA neighborhood is for the convenience of computation. It is different from the mathematical neighborhood with respect to CD function. For instance, considering the uniform design  $U_{18}(3^7)$  recorded on the website mentioned before, Figure 2 gives the distributions of CD values of designs in different neighborhoods. The right box-plot in Figure 2 plots the CD values of TA neighborhoods of  $U_{18}(3^7)$ . The left box-plot is for the designs derived by level permutation on randomly chosen one column of  $U_{18}(3^7)$ . The CD value of TA neighborhoods may vary from each other in a great amount, compared to level permuted designs. Hence, this definition of neighborhood is not feasible for continuous uniform designs.

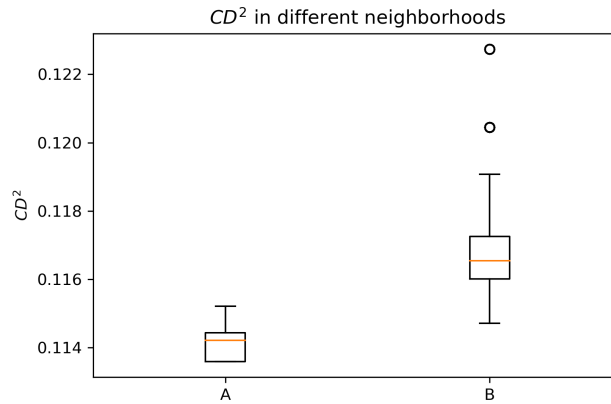


Figure 2: The CD distributions in different neighborhoods of  $U_{18}(3^7)$ .

A: The box-plot of  $CD^2$  in level permutation of one randomly chosen column of  $U_{18}(3^7)$ .

B: The box-plot of  $CD^2$  in level-permutation neighborhood

### 3 Coordinate Descent Algorithms with TA Initialization

Coordinate descent algorithms are a class of large-scale optimization algorithms that are feasible for various objective functions including non-smooth and non-convex ones. They have been successfully implemented on the problems in various modern applications such as machine learning and large-scale computational statistics. For some structured problems, coordinate descent algorithms have shown advantage on computation speed and convergence proof over traditional algorithms, such as gradient descent (GD), refer to Shi et al. (2016). A comprehensive introduction with applications to coordinate descent variants has been elaborated by Wright (2015) and Shi et al. (2016). In this paper, three coordinate descent algorithms are introduced and discussed on their performance in constructing UDs.

Recall in (6) that constructing a uniform design under CD is an optimization problem with non-convex objective function,

$$y = \arg \min_{\mathcal{P}=[0,1]^{ns}} g(x_1, \dots, x_p),$$

where the objective function  $g(x_1, \dots, x_p)$  indicating CD in (4) has the second derivative, and  $p = ns$ . In traditional gradient optimization algorithm, there are two possible actions in each iteration. Coordinate descent is a simple but efficient non-gradient optimization algorithm. The gradient optimization algorithm seeks for the minimum value of the function along the direction of the most rapid descent. However, coordinate descent minimizes the value of the objective function along the coordinate gradient in each step.

### 3.1 *Coordinate Gradient Descent (CGD)*

To construct a UD,  $U_n(q^s)$ , the optimization problem can be regarded as an  $s$ -dimensional problem with  $n$  points on  $[0, 1]^s$ . An  $n \times s$  uniform design matrix can be viewed as  $n$  design points each having  $s$  dimension. Coordinate gradient descent is to adjust the position of each design point in each dimension so that the whole design point set can be more uniformly distributed in the domain. Figure 3 visualizes the design points during the optimization process. Figure 4 presents the design points of  $U_9(9^4)$  from any two-dimensional projection points. The visualization figures may help us comprehend the objective uniformity measure CD adopted in this paper. The figures indicate that the whole design points become centrally aggregated after coordinate descent. The following algorithm is the basic coordinate gradient descent method.

---

**Algorithm 1** Coordinate Gradient Descent(CGD)

---

- 1: Given  $n, s$
  - 2: Initialization  $X^0$  and choose  $\epsilon$ , the step size  $\delta$  and the maximum epoch  $M$ .
  - 3: Create cd list and matrix list
  - 4: **for** each  $m \in [0, M]$  **do**
  - 5:     **for** each  $i \in [0, n]$  **do**
  - 6:         **for** each  $j \in [0, s]$  **do**
  - 7:             Calculate the Coordinate Gradient descent,  $g = \frac{dCD^2(X^m)}{dx_{ij}^m}$
  - 8:              $x_{ij}^{m+1} = x_{ij}^m + g * \delta$
  - 9:         **end for**
  - 10:     **end for**
  - 11:     if  $|CD^2(X^{m+1}) - CD^2(X^m)| < \epsilon$ , then break the for-loop
  - 12: **end for**
-

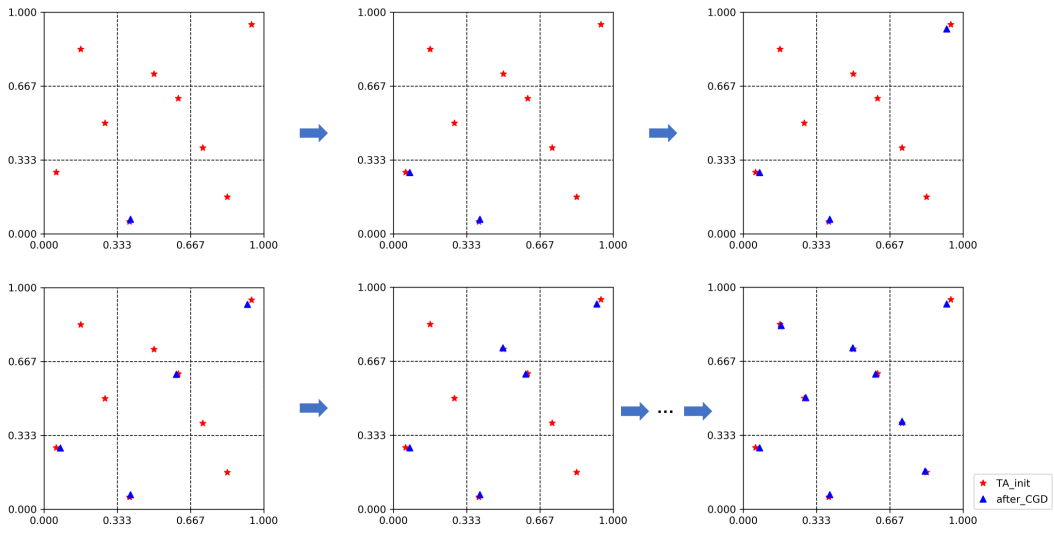


Figure 3: Visualization of design points during the optimization process

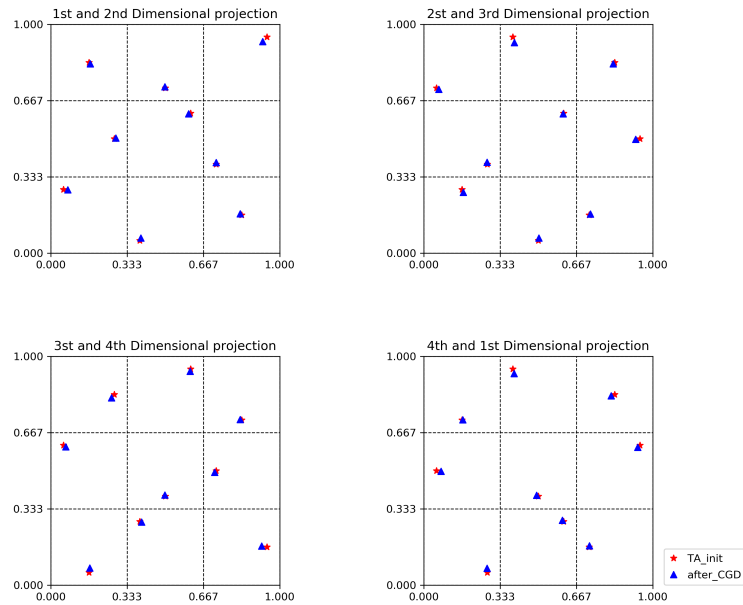


Figure 4: Design points from any two-dimensional projection points

### 3.2 Coordinate Zero-gradient (CZG)

Since the coordinate gradient in Algorithm 1,  $g = \frac{dCD^2(X^m)}{dx_{ij}^m}$ , is known, we can set  $g = 0$  to find the coordinate value while fixing other coordinate values.

$$\begin{aligned}
\frac{dCD^2(\mathcal{P})}{dx_{ij}} &= -\frac{2}{n} \left\{ \prod_{q \neq j}^s \left[ 1 + \frac{1}{2}|x_{iq} - \frac{1}{2}| - \frac{1}{2}(x_{iq} - \frac{1}{2})^2 \right] \right\} \\
&\times \left[ \frac{1}{2} \text{sgn}(x_{ij} - \frac{1}{2}) - (x_{ij} - \frac{1}{2}) \right] \\
&+ \frac{1}{n^2} \prod_{q \neq j}^s \frac{1}{2} (1 + |x_{iq} - \frac{1}{2}|) \text{sgn}(x_{ij} - \frac{1}{2}) \\
&+ \frac{2}{n^2} \sum_{k \neq i}^n \left\{ \prod_{q \neq j}^s \left[ 1 + \frac{1}{2}|x_{iq} - \frac{1}{2}| + \frac{1}{2}|x_{kq} - \frac{1}{2}| - \frac{1}{2}|x_{iq} - x_{kq}| \right] \right. \\
&\times \left. \left[ \frac{1}{2} \text{sgn}(x_{ij} - \frac{1}{2}) - \frac{1}{2} \text{sgn}(x_{ij} - x_{kj}) \right] \right\}, \tag{7}
\end{aligned}$$

where the sgn function is:

$$\text{sgn}(x) = \begin{cases} 1, & x < 0, \\ 0, & x = 0, \\ -1, & x > 0. \end{cases} \tag{8}$$

The coordinate value,  $x_{ij}$ , can be derived through taking  $\frac{dCD^2(\mathcal{P})}{dx_{ij}} = 0$ . However, some of  $x_{ij}$  in sgn function can not be solved through explicit expression. Here we adopt recursion with an initialization, denoted as  $x_{ij}^0$ , and a maximum number of iterations,  $T$ , while other coordinate values  $\{x_{kq}, k \neq i, q \neq j\}$ , are fixed. The recursive formula is given as

$$x_{ij}^t = \frac{A}{B} + \frac{1}{2}, \tag{9}$$

where

$$\begin{aligned}
A &= -\frac{2}{n} \left\{ \prod_{q \neq j}^s \left[ 1 + \frac{1}{2} |x_{iq} - \frac{1}{2}| - \frac{1}{2} (x_{iq} - \frac{1}{2})^2 \right] \right\} \times \frac{1}{2} \text{sgn}(x_{ij}^{t-1} - \frac{1}{2}) \\
&+ \frac{1}{n^2} \prod_{q \neq j}^s \frac{1}{2} (1 + |x_{iq} - \frac{1}{2}|) \text{sgn}(x_{ij}^{t-1} - \frac{1}{2}) \\
&+ \frac{2}{n^2} \sum_{k \neq i}^n \left\{ \prod_{q \neq j}^s \left[ 1 + \frac{1}{2} |x_{iq} - \frac{1}{2}| + \frac{1}{2} |x_{kq} - \frac{1}{2}| - \frac{1}{2} |x_{iq} - x_{kq}| \right] \right. \\
&\times \left. \left[ \frac{1}{2} \text{sgn}(x_{ij}^{t-1} - \frac{1}{2}) - \frac{1}{2} \text{sgn}(x_{ij}^{t-1} - x_{kj}) \right] \right\} \tag{10}
\end{aligned}$$

and

$$B = -\frac{2}{n} \prod_{q \neq j}^s \left[ 1 + \frac{1}{2} |x_{iq} - \frac{1}{2}| - \frac{1}{2} (x_{iq} - \frac{1}{2})^2 \right] \tag{11}$$

for  $t \in [0, T]$ . Through plenty of experiments,  $T = 1$  is enough for getting good results.

---

**Algorithm 2** Coordinate zero-gradient

---

- 1: Given  $n, s$
  - 2: Initialization  $X^0$  and choose  $\epsilon$  and the maximum epoch  $M$ .
  - 3: Create cd list and matrix list
  - 4: **for** each  $m \in [0, M]$  **do**
  - 5:     **for** each  $i \in [0, n]$  **do**
  - 6:         **for** each  $j \in [0, s]$  **do**
  - 7:             Let  $\{x_{kl}^m, k \neq i, l \neq j\}$  be fixed. Calculate  $\hat{x}_{ij}^m$  such that Coordinate Gradient descent,  $\frac{dCD^2(\mathcal{P})}{d\hat{x}_{ij}^m} = 0$ .
  - 8:              $x_{ij}^{m+1} = \hat{x}_{ij}^m$
  - 9:         **end for**
  - 10:     **end for**
  - 11:     if  $|CD^2(X^{m+1}) - CD^2(X^m)| < \epsilon$ , then break the for-loop
  - 12: **end for**
- 

In our experiments, the coordinate zero-gradient method is advantaged in computation speed. For the same optimization task, it takes several minutes through coordinate gradient descent method but several seconds through coordinate zero-gradient method. However, even though the final optimization result is good enough, the CD values during the optimization process is unstable. For instance, sometimes

there may be violent fluctuations of the CD values.

### 3.3 *Coordinate Descent with Fixed Step Size (CDFSS)*

Considering the limit of minimum unit of variables in practical experiments, coordinate descent with fixed step size are suitable under such circumstances. The idea of this method is to replace the coordinate gradient with  $\{-1, 1\}$  and the step size can be set as the minimum unit of variables. In each step, the coordinate with the rapidest descent will be chosen. The algorithm will be stopped until there is no further descent in any coordinate.

This method can be easily applied in the experiments with minimum unit due to the equipment or technology limitations. For example, one of the variable, temperature, in the industry experiment is from 0 to T. Due to the limitations of temperature detection and control technology, the minimum unit is 0.1 degree. With CDFSS, the step size of the variable can be set as  $\frac{0.1}{T-0}$ . Similarly for other variables, the step size can be set different values according to the corresponding limitations. Thus, the resulted uniform design is feasible under practical experimental requirements.

---

**Algorithm 3** Coordinate Descent with Fixed Step Size

---

- 1: Given  $n, s$
  - 2: Initialization  $X^0$  and choose the step size in each column  $\{\delta_j, j \leq s\}$  and the maximum epoch  $M$ .
  - 3: Create CD list and matrix list
  - 4: **for** each  $m \in [0, M)$  **do**
  - 5:     **for** each  $i \in [0, n)$  **do**
  - 6:         **for** each  $j \in [0, s]$  **do**
  - 7:             **for** each  $a \in \{-1, 1\}$  **do**
  - 8:                  $\hat{X}$  be the copy of  $X^m$
  - 9:                  $\hat{x}_{ij} = \hat{x}_{ij} + a * \delta_j$
  - 10:                 Calculate  $cd = CD^2(\hat{X})$  and put  $cd$  into  $cd$  list and put  $\hat{X}$  into matrix list
  - 11:             **end for**
  - 12:         **end for**
  - 13:     **end for**
  - 14:     Find the matrix with minimum CD in matrix list and if the CD is smaller than the CD of  $X^m$ , then let  $X^{m+1}$  be such matrix, otherwise break the for-loop
  - 15: **end for**
-

Actually, in the experiments, these three algorithms may get different results with the same initialization. With the same initialization, the aforementioned three algorithms are conducted respectively. We present the CD values in Table 1. Table 1 shows that the final uniform designs of these algorithms may be different due to the complexity of non-convex high dimensional optimization. But using better initialization ( $U_{18}(18^7)$  on the website) facilitates the optimization process.

Table 1:  $CD^2$  of different algorithms with the same initialization

Algorithm \ Initialization	Website	$X_{ij} \sim U(0, 1)$
GD	0.033972	0.052300
CGD	0.033972	0.041678
CZG	0.033972	0.052690
CDFSS	0.033972	0.042079

### 3.4 TA Initialization

Due to the non-convexity of  $CD^2$  in (4), the initialization is significant in the gradient-based methods. With different initialization, various local minimum will be achieved by using the same coordinate descent algorithm. For example, when constructing  $U_{18}^{new}(18^7)$  through different initial designs, coordinate gradient descent obtains different results shown in Table 2.

Table 2: Coordinate gradient descent with different initialization

Initialization type	$CD^2$
$X_{ij} \sim U(0, 1)$	0.041678
$X_{ij} \sim N(0.5, 0.1^2)$	0.061949
$X_{ij} = 0$	0.041114
$X_{ij} = 1$	0.041227
$U_{18}(18^7)$ on website	0.033972

TA algorithm has successfully obtained many uniform designs over the U-type lattice point domain on the website mentioned above. Hence, intuitively we adopt the uniform design derived by TA algorithm as the initialization. Then subsequently, we conduct the coordinate descent methods to optimize the uniform designs over a



continuous domain,  $[0, 1]^s$ . Table 3 presents the CD values of uniform designs derived by TA over a U-type domain and by TA+CGD over a continuous domain. The CD values can be further improved over a continuous domain through coordinate descent methods, compared to the existing UDs on the website.

Table 3: CD values of uniform designs through TA and TA+CGD

Algorithms	$U_{18}(18^7)$	$U_{27}(27^{13})$
TA	0.035403	0.228455
TA + CGD	0.033972	0.198073

Table 4:  $U_{18}^{new}(18^7)$  obtained by TA+CGD

0.9080	0.5238	0.6906	0.8001	0.7509	0.3578	0.9071
0.3050	0.5838	0.6351	0.0531	0.6986	0.7447	0.1393
0.7475	0.2567	0.4738	0.2078	0.9052	0.8544	0.6415
0.9457	0.1462	0.3609	0.4796	0.3579	0.6288	0.0542
0.4704	0.6925	0.5757	0.9079	0.1977	0.2049	0.0972
0.1438	0.4809	0.0946	0.2525	0.0549	0.5210	0.2979
0.5264	0.0986	0.8501	0.1441	0.1533	0.4260	0.7990
0.3570	0.0529	0.1464	0.5804	0.8045	0.2527	0.4264
0.0957	0.7482	0.9468	0.5135	0.8528	0.5862	0.5889
0.6366	0.4197	0.0528	0.9471	0.5825	0.6931	0.7531
0.0546	0.3076	0.4149	0.6973	0.3062	0.0959	0.6922
0.2009	0.1964	0.7458	0.8505	0.4748	0.9032	0.3564
0.7971	0.8605	0.8011	0.6355	0.0960	0.7947	0.4694
0.4159	0.6462	0.2524	0.4225	0.2570	0.9456	0.9456
0.5711	0.9058	0.2994	0.7430	0.9456	0.4756	0.2040
0.2435	0.9512	0.5211	0.3061	0.5330	0.3026	0.8508
0.6876	0.3689	0.9043	0.3633	0.6321	0.0539	0.2502
0.8534	0.7923	0.1928	0.0974	0.4286	0.1500	0.5260

To further explore the performance of new uniform designs, we implement them on several computer experiments in the next section. In these case studies, we use Kriging modeling technique to obtain an approximate model for responses and factors. We evaluate the mean squared errors (MSE) when predicting untried points through the approximate models trained by the new uniform designs, compared with the ones recorded on the website, and the Latin hypercube sampling.

Table 5:  $U_{27}^{new}(27^{13})$  obtained by TA+CGD

0.0971	0.8438	0.2913	0.5290	0.7735	0.4409	0.8424	0.6708	0.4005	0.1238	0.3293	0.6793	0.8683
0.5663	0.8711	0.7423	0.3992	0.1332	0.1908	0.1838	0.3580	0.5025	0.8424	0.5971	0.7083	0.0939
0.7020	0.0962	0.2268	0.1853	0.5957	0.3299	0.5591	0.0915	0.1942	0.4693	0.6391	0.7802	0.7763
0.1914	0.5124	0.6684	0.7741	0.5287	0.1272	0.2272	0.2965	0.3338	0.2203	0.8354	0.2634	0.8097
0.2906	0.2188	0.4044	0.3498	0.6775	0.1570	0.9011	0.1962	0.8988	0.5647	0.4023	0.3885	0.1243
0.4771	0.1907	0.8427	0.9289	0.7377	0.9084	0.0971	0.5278	0.2559	0.4013	0.4324	0.7423	0.5594
0.3673	0.1224	0.8728	0.6715	0.3999	0.2237	0.6704	0.8715	0.6986	0.8150	0.2553	0.5226	0.7389
0.8424	0.4354	0.9068	0.8085	0.9281	0.4679	0.7395	0.1242	0.4656	0.7069	0.5278	0.1253	0.4302
0.0717	0.1596	0.2587	0.2915	0.2922	0.5324	0.3007	0.5610	0.5250	0.9289	0.8047	0.0925	0.5224
0.2272	0.6788	0.5259	0.7056	0.0705	0.8810	0.6402	0.1554	0.6313	0.6011	0.9295	0.6398	0.6283
0.9267	0.7367	0.8156	0.3238	0.2645	0.5657	0.3593	0.2191	0.1246	0.0966	0.3680	0.5100	0.6731
0.9006	0.3594	0.1018	0.4724	0.8127	0.2550	0.1526	0.7021	0.6665	0.2897	0.9045	0.5622	0.3623
0.6695	0.0708	0.4881	0.6381	0.5080	0.8414	0.4007	0.9288	0.4352	0.0711	0.6766	0.3326	0.0710
0.5170	0.4010	0.4748	0.1214	0.0934	0.4096	0.0724	0.7373	0.2922	0.6378	0.1547	0.3624	0.9275
0.1574	0.3288	0.6032	0.4884	0.8388	0.7119	0.4358	0.2642	0.0962	0.8977	0.0973	0.5941	0.2872
0.6397	0.8051	0.1902	0.9022	0.7080	0.5996	0.4721	0.4047	0.8367	0.8721	0.7358	0.4241	0.9042
0.8098	0.7682	0.6383	0.7497	0.5623	0.3728	0.3233	0.7705	0.9292	0.5323	0.1828	0.8078	0.2576
0.4356	0.9014	0.7820	0.2190	0.6455	0.6712	0.8026	0.8402	0.2229	0.5137	0.8732	0.2930	0.3339
0.5292	0.2573	0.1643	0.8350	0.2219	0.6356	0.7776	0.3306	0.5549	0.1957	0.1271	0.8760	0.3938
0.3232	0.5606	0.3683	0.2547	0.9073	0.8088	0.2573	0.9027	0.7356	0.6824	0.5189	0.9025	0.6990
0.1306	0.4634	0.9265	0.0734	0.3654	0.4859	0.5235	0.4446	0.8092	0.1592	0.7133	0.8388	0.2217
0.4013	0.9279	0.3244	0.5670	0.4259	0.7460	0.1239	0.0721	0.7729	0.3316	0.2306	0.1871	0.4684
0.8678	0.5964	0.0736	0.0967	0.4722	0.9262	0.7000	0.4762	0.3608	0.7794	0.2910	0.4719	0.1625
0.7417	0.5304	0.4385	0.6016	0.3333	0.0932	0.9281	0.5975	0.0718	0.7427	0.7742	0.9281	0.5089
0.7788	0.3003	0.7021	0.4343	0.1600	0.7792	0.8683	0.6321	0.8693	0.3659	0.5660	0.2166	0.8376
0.2576	0.6397	0.1321	0.8754	0.1864	0.2929	0.5135	0.8070	0.1546	0.4325	0.4745	0.1554	0.1941
0.6064	0.6963	0.5617	0.1565	0.8705	0.0711	0.5982	0.5135	0.5994	0.2536	0.0715	0.0715	0.5914

## 4 Modeling Performance of Uniform designs over Continuous Domain

The question is requested whether the new uniform designs with smaller CD on the continuous domain has better performance in modeling. We apply the new uniform designs in several computer experiments as case studies. There are many modeling techniques among which we adopt Kriging modeling technique in this study. Fang et al. (2005) gave an elaborate introduction to Kriging models.

**Definition 3.** Suppose that  $\mathbf{x}_i$ ,  $i = 1, \dots, n$  are design points over an  $s$ -dimensional experimental domain, and  $y_i = y(\mathbf{x}_i)$  is the corresponding output. The universal Gaussian Kriging model is defined as

$$y(\mathbf{x}) = \sum_{j=0}^L \beta_j B_j(\mathbf{x}) + z(\mathbf{x}),$$

where the set of  $B_j$  is a chosen polynomial basis over the design region and  $z(\mathbf{x})$  is a Gaussian process. The ordinary Kriging model is the most commonly used in practice, defined as

$$y(\mathbf{x}) = \mu + z(x),$$

where  $\mu$  is the overall mean of  $y$ .

DACE package in MATLAB is employed for Kriging modeling. There are several candidate basis in this package, such as *Poly0* representing ordinary Kriging models, *Poly1* representing first-order polynomial function as basis, and *Poly2* representing second-order polynomial function as basis. We evaluate the modeling performance through comparing the prediction MSE on untried 1000 points of Kriging models trained by the new uniform designs and the recorded ones in the website. The MSE is defined as follows.

$$MSE = \frac{1}{M} \sum_{m=1}^M (y_m - \hat{y}_m)^2.$$

Since Latin hypercube sampling (LHS) has been popular in computer experiments, we also provide the prediction MSE of the Kriging models trained by LHS and mid-point LHS (MLHS), defined in Definition 5. Since each LHS or MLHS is a random sample, we generate ten LHS or MLHS each time and conduct Kriging modeling respectively. Subsequently, we present the average prediction MSE of each Kriging model trained by these ten LHS or MLHS, denoted as Avg. LHS or Avg. MLHS in Table 7 and 8.

**Definition 4.** A Latin hypercube design (LHD) with  $n$  runs and  $s$  factors, denoted by  $LHD(n, s)$ , is an  $n \times s$  matrix, in which each column is a random permutation of  $1, 2, \dots, n$ .

**Definition 5.** Let  $\pi_j(1), \dots, \pi_j(n)$ ,  $j = 1, \dots, s$ , denote the  $s$  permutations of  $LHD(n, s)$ . Take mutually independent  $ns$  uniform random variables  $U_k^j \sim U(0, 1)$ ,

$k = 1, \dots, n, j = 1, \dots, s$ . Let  $\mathbf{x}_k = (x_k^1, \dots, x_k^s)$ , where  $x_k^j = \frac{\pi_j(k) - U_k^j}{n}$ ,  $k = 1, \dots, n$ ,  $j = 1, \dots, s$ . Then  $\mathbf{D}_n = \{\mathbf{x}_1, \dots, \mathbf{x}_n\}$  is a LHS and denoted by  $LHS(n, s)$ . If for each  $x_k^j$ , we fix at a mid-point instead of a random number, that is  $x_k^j = \frac{\pi_j(k) - 0.5}{n}$ ,  $\mathbf{D}_n$  is a mid-point LHS, denoted as  $MLHS$ .

## 4.1 Wood Model

A wood function is notorious due to its difficulty on optimization, defined by

$$Y = 100(x_1^2 - x_2)^2 + (1 - x_1)^2 + 90(x_4 - x_3^2)^2 + (1 - x_3)^2 + 10.1((x_2 - 1)^2 + (x_4 - 1)^2) + 19.8(x_2 - 1)(x_4 - 1),$$

for  $(x_1, x_2, x_3, x_4) \in [-2, 2]^4$ . The global minimum is at  $x^* = [1, 1, 1, 1]$  with  $Y^* = 0$ .

We apply several new uniform designs over continuous domain, denoted as  $U_n^{new}(n^s)$ , and the corresponding recorded ones,  $U_n(n^s)$  on the website respectively into wood model, in which 9-run and 16-run designs shown in Table 6.

Table 6:  $U_9(9^4)$ ,  $U_9^{new}(9^4)$ ,  $U_{16}(16^4)$ , and  $U_{16}^{new}(16^4)$  in wood model

$U_9(9^4)$				$U_9(9^4) \in [-2, 2]^4$				$U_9^{new}(9^4) \in [0, 1]^4$				$U_9^{new}(9^4) \in [-2, 2]^4$			
4	1	7	5	-0.5	-2	1	0	0.3942	0.0690	0.7114	0.5978	-0.4232	-1.7242	0.8457	0.3912
1	3	4	3	-2	-1	-0.5	-1	0.0743	0.2762	0.3966	0.2761	-1.7030	-0.8953	-0.4136	-0.8957
9	9	5	4	2	2	0	-0.5	0.9303	0.7215	0.6060	0.3940	1.7214	0.8861	0.4240	-0.4240
6	6	6	9	0.5	0.5	0.5	2	0.6086	0.5114	0.4910	0.7172	0.4344	0.0456	-0.0360	0.8689
5	7	2	1	0	1	-1.5	-2	0.5000	0.9207	0.2751	0.0793	0.0000	1.6830	-0.8997	-1.6830
2	8	8	7	-1.5	1.5	1.5	1	0.1758	0.8242	0.8242	0.8242	-1.2969	1.2969	1.2969	1.2969
3	5	1	6	-1	0	-2	0.5	0.2837	0.6065	0.0658	0.5000	-0.8653	0.4260	-1.7370	0.0000
8	2	3	8	1.5	-1.5	-1	1.5	0.8208	0.1875	0.1792	0.9065	1.2833	-1.2501	-1.2833	1.6262
7	4	9	2	1	-0.5	2	-1.5	0.7127	0.3945	0.9214	0.1705	0.8509	-0.4220	1.6858	-1.3181
$U_{16}(16^4)$				$U_{16}(16^4) \in [-2, 2]^4$				$U_{16}^{new}(16^4) \in [0, 1]^4$				$U_{16}^{new}(16^4) \in [-2, 2]^4$			
1	10	4	6	-2.00	0.40	-1.20	-0.67	0.4678	0.6593	0.4717	0.7195	-0.1290	0.6370	-0.1134	0.8778
2	4	13	15	-1.73	-1.20	1.20	1.73	0.2873	0.3469	0.0440	0.7769	-0.8510	-0.6126	-1.8242	1.1074
3	13	10	10	-1.47	1.20	0.40	0.40	0.1599	0.7847	0.5913	0.5975	-1.3606	1.1386	0.3650	0.3898
4	8	7	1	-1.20	-0.13	-0.40	-2.00	0.0415	0.5965	0.2213	0.3425	-1.8342	0.3858	-1.1150	-0.6302
5	6	1	2	-0.93	-0.67	-2.00	-1.73	0.7808	0.0927	0.3474	0.6514	1.1230	-1.6294	-0.6106	0.6054
6	15	15	4	-0.67	1.73	1.73	-1.20	0.2165	0.4656	0.4057	0.0389	-1.1342	-0.1378	-0.3774	-1.8446
7	1	11	7	-0.40	-2.00	0.67	-0.40	0.7252	0.7091	0.9508	0.0981	0.9006	0.8362	1.8030	-1.6078
8	16	8	14	-0.13	2.00	-0.13	1.47	0.3397	0.9060	0.7747	0.2254	-0.6414	1.6238	1.0986	-1.0986
9	3	3	3	0.13	-1.47	-1.47	-1.47	0.8519	0.5300	0.7172	0.8348	1.4074	0.1198	0.8686	1.3390
10	7	16	9	0.40	-0.40	2.00	0.13	0.6437	0.9514	0.2860	0.9514	0.5746	1.8054	-0.8562	1.8054
11	11	5	16	0.67	0.67	-0.93	2.00	0.4103	0.0373	0.6566	0.4060	-0.3590	-1.8510	0.6262	-0.3762
12	12	12	2	0.93	0.93	0.93	-1.73	0.5944	0.4045	0.8392	0.5308	0.3774	-0.3822	1.3566	0.1230
13	2	6	11	1.20	-1.73	-0.67	0.67	0.9013	0.8316	0.0971	0.4668	1.6050	1.3262	-1.6118	-0.1330
14	14	2	8	1.47	1.47	-1.73	-0.13	0.9600	0.2836	0.5329	0.2779	1.8398	-0.8658	0.1314	-0.8886
15	9	14	13	1.73	0.13	1.47	1.20	0.5341	0.2096	0.1563	0.1535	0.1362	-1.1618	-1.3750	-1.3862
16	5	9	5	2.00	-0.93	0.13	-0.93	0.1032	0.1681	0.8969	0.8969	-1.5874	-1.3278	1.5874	1.5874

Table 7: The  $\sqrt{MSE}$  of Kriging models in wood model

	$U_9(9^4)$	$U_9^{new}(9^4)$	Avg. <i>LHS</i>	Avg. <i>MLHS</i>
<i>Poly0</i>	957.9618	826.0637	816.8131	805.1325
<i>Poly1</i>	878.1982	695.0498	877.2432	847.6947
	$U_{16}(16^4)$	$U_{16}^{new}(16^4)$	Avg. <i>LHS</i>	Avg. <i>MLHS</i>
<i>Poly0</i>	829.4668	743.3496	672.0404	725.3436
<i>Poly1</i>	779.9872	722.6574	667.8994	765.7914
	$U_{18}(18^4)$	$U_{18}^{new}(18^4)$	Avg. <i>LHS</i>	Avg. <i>MLHS</i>
<i>Poly0</i>	691.7101	668.6842	731.2896	685.1813
<i>Poly1</i>	618.7809	587.3990	717.9110	711.0604
	$U_{27}(27^4)$	$U_{27}^{new}(27^4)$	Avg. <i>LHS</i>	Avg. <i>MLHS</i>
<i>Poly0</i>	2768.7	543.0675	568.6300	558.2930
<i>Poly1</i>	1743.9	534.7528	653.5637	603.9952

Besides Table 6, we also implement 18-run and 27-run designs, LHS, and MLHS. We use the above mentioned designs with *Poly0* and *Poly1* bases to develop Kriging models. For convenience of reading,  $\sqrt{MSE}$  are calculated and listed in Table 7. It is obvious that new uniform designs over continuous domain perform better than recorded ones in wood model.

## 4.2 *Six-hump Camelback Model*

The function with six-hump camelback surface and six local minima is defined by

$$Y = 4x_1^2 - 2.1x_1^4 + \frac{1}{3}x_1^6 + x_1x_2 - 4x_2^2 + 4x_2^4, (x_1, x_2) \in [-3, 3] \times [-2, 2].$$

The global minimum is  $Y^* = -1.03$ , when  $\mathbf{x}^* = [0.09, -0.71]$  or  $[-0.09, 0.71]$ . Figure 5 presents the surface of the six-hump Camelback function on  $[-2, 2] \times [-1, 1]$ . Tabel 8 presents the prediction MSE of Kriging models developed from the 16-run and 27-run designs, LHS and MLHS with *Poly0*, *Poly1* and *Poly2* bases respectively. The new uniform designs,  $U_{16}^{new}(16^2)$  and  $U_{27}^{new}(27^2)$ , perform better in six-hump camelback model as well.

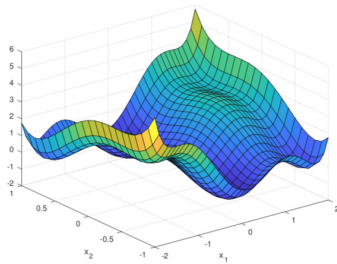


Figure 5: The surface of six-hump camelback function

Table 8: The MSE of Kriging models in six-hump camelback model

	$U_{16}(16^2)$	$U_{16}^{new}(16^2)$	Avg. <i>LHS</i>	Avg. <i>MLHS</i>
<i>Poly0</i>	316.0265	210.8945	383.1213	338.0651
<i>Poly1</i>	316.0265	210.8945	426.6880	380.9689
<i>Poly2</i>	253.8087	182.3029	215.1144	221.8797
	$U_{27}(27^2)$	$U_{27}^{new}(27^2)$	Avg. <i>LHS</i>	Avg. <i>MLHS</i>
<i>Poly0</i>	159.2230	178.3153	193.8387	176.9656
<i>Poly1</i>	159.7014	178.9219	176.9656	182.0625
<i>Poly2</i>	78.9778	93.0508	164.9395	115.1672

## 5 Conclusion

To yield a new uniform design over continuous experimental domain under the measurement of the centered  $L_2$ -discrepancy (CD), that is a high dimensional ( $p = ns$ , where  $n$  is the number of runs and  $s$  the number of factors) non-convex optimization problem, we adopt three coordinate descent algorithms with a U-type initialization derived by TA algorithms. It turns out that the CD values of UDs over continuous domain has been reduced considerably.

The Algorithms 1, 2, and 3 are three coordinate descent variants, performing similarly in our case. In Figure 6, we give the trace plot of CD in the above three algorithms. Coordinate zero-gradient (Algorithm 2) is the fastest algorithm among them. As for coordinate descent with fixed step size (Algorithm 3), it does not need the coordinate gradient. Similar to gradient descent, coordinate gradient descent is stable in each step. In addition, coordinate gradient descent adjusts the position of each design point in each dimension. Compared with gradient descent

algorithm, coordinate descent algorithms are simpler and cheaper. Moreover, each step in coordinate descent is meaningful, which can be visualized during the optimization process. The visualization is helpful for comprehending uniformity and the optimization process. Furthermore, it is convenient to be generalized into practical implementation on the experiments with required minimum unit of factors.

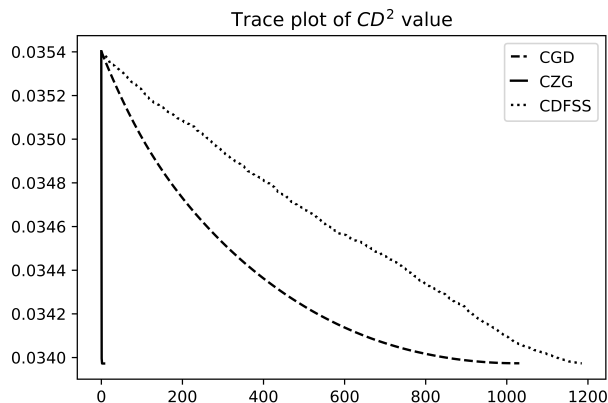


Figure 6:  $CD^2$  trace plot of three algorithms

Subsequently, to evaluate the new UD<sub>s</sub> over continuous domain, we compare the modeling performance of the new designs with the recorded UD<sub>s</sub> on the website, as well as Latin hypercube sampling in two computer experiments as illustrative instances. The prediction MSE is adopted as evaluation criteria. In this paper, we take Kriging modeling technique to yield the metamodels, that may affect the MSE as well. Nevertheless, it indicates that the new uniform designs are advantaged on modeling in computer experiments. Uniform designs over continuous domain is promising since designs with continuous factors become feasible and in demand with the improvement of computational ability.

## 6 Acknowledgement

This work was partially supported by the Zhuhai Premier Discipline Grant; Guangdong Natural Science Foundation under Grant No. 2018A0303130231; and BNU-

HKBU United International College under Grant R202108. We thank Dr. Peng Heng for his support.

## References

- Chipman, J. S. and Winker, P. (1995). Optimal industrial classification by threshold accepting. *Control and Cybernetics*, 24:477–494.
- Dueck, G. and Scheuer, T. (1990). Threshold accepting: a general purpose optimization algorithm appearing superior to simulated annealing. *Journal of Computational Physics*, 90(1):161–175.
- Dueck, G. and Winker, P. (1992). New concepts and algorithms for portfolio choice. *Applied Stochastic Models and Data Analysis*, 8(3):159–178.
- Fang, K. T. (1980). The uniform design: Application of number-theoretic methods in experimental design. *Acta Mathematicae Applicatae Sinica*, 3(4):363–372.
- Fang, K. T., Ke, X., and Elsayah, A. M. (2017). Construction of uniform designs via an adjusted threshold accepting algorithm. *Journal of Complexity*, 43:28–37.
- Fang, K. T., Li, R., and Sudjianto, A. (2005). *Design and Modeling for Computer Experiments*. CRC press.
- Fang, K. T., Liu, M. Q., Qin, H., and Zhou, Y. D. (2018). *Theory and Application of Uniform Experimental Designs*. Science Press and Springer.
- Hickernell, F. (1998). A generalized discrepancy and quadrature error bound. *Mathematics of Computation*, 67(221):299–322.
- Hua, L. K. and Wang, Y. (1981). *Applications of Number Theory to Numerical Analysis*. Springer and Science Press.



- Kirkpatrick, S. (1984). Optimization by simulated annealing: Quantitative studies. *Journal of Statistical Physics*, 34(5-6):975–986.
- McKay, M. D., Beckman, R. J., and Conover, W. J. (1979). A comparison of three methods for selecting values of input variables in the analysis of output from a computer code. *Technometrics*, 21:239–245.
- Ruder, S. (2016). An overview of gradient descent optimization algorithms. *arXiv preprint arXiv:1609.04747*.
- Shi, H. J. M., Tu, S., Xu, Y., and Yin, W. (2016). A primer on coordinate descent algorithms. *arXiv preprint arXiv:1610.00040*.
- Wang, Y. and Fang, K. T. (1981). A note on uniform distribution and experimental design. *Kexue Tongbao (Chinese Science Bulletin)*, (26):485–489.
- Winker, P. (1994). The tuning of the threshold accepting heuristic for travelling salesman problems. In *Sonderforschungsbereich*, volume 178. Universität Konstanz.
- Winker, P. and Fang, K. T. (1997). Application of threshold-accepting to the evaluation of the discrepancy of a set of points. *SIAM Journal on Numerical Analysis*, 34(5):2028–2042.
- Winker, P. and Fang, K. T. (1998). Optimal u-type designs. In *Monte Carlo and Quasi-Monte Carlo Methods 1996*, pages 436–448. Springer.
- Wright, S. J. (2015). Coordinate descent algorithms. *Mathematical Programming*, 151(1):3–34.
- Zhou, Y. D., Fang, K. T., and Ning, J. H. (2013). Mixture discrepancy for quasi-random point sets. *Journal of Complexity*, 29(3-4):283–301.